



OPEN ACCESS

EDITED BY

Prasanta Kumar Dash,
University of Nebraska Medical Center,
United States

REVIEWED BY

Olfat Ali Hammam,
Theodor Bilharz Research Institute,
Egypt
Yifan Bao,
Johnson & Johnson, United States

*CORRESPONDENCE

Shaogui Wang,
✉ wangshaogui@gzucm.edu.cn
Guifang Zhang,
✉ zhanggfg@gzucm.edu.cn
Lin An,
✉ anlin@gzucm.edu.cn

SPECIALTY SECTION

This article was submitted to
Ethnopharmacology,
a section of the journal
Frontiers in Pharmacology

RECEIVED 13 September 2022
ACCEPTED 05 December 2022
PUBLISHED 14 December 2022

CITATION

Wu B, Huang L, Wang Y, Zeng L, Lin Y,
Li J, Wang S, Zhang G and An L (2022),
Yao medicine *Amydrium hainanense*
suppresses hepatic fibrosis by
repressing hepatic stellate cell activation
via STAT3 signaling.
Front. Pharmacol. 13:1043022.
doi: 10.3389/fphar.2022.1043022

COPYRIGHT

© 2022 Wu, Huang, Wang, Zeng, Lin, Li,
Wang, Zhang and An. This is an open-
access article distributed under the
terms of the [Creative Commons
Attribution License \(CC BY\)](https://creativecommons.org/licenses/by/4.0/). The use,
distribution or reproduction in other
forums is permitted, provided the
original author(s) and the copyright
owner(s) are credited and that the
original publication in this journal is
cited, in accordance with accepted
academic practice. No use, distribution
or reproduction is permitted which does
not comply with these terms.

Yao medicine *Amydrium hainanense* suppresses hepatic fibrosis by repressing hepatic stellate cell activation via STAT3 signaling

Bingmin Wu, Lan Huang, Yange Wang, Lishan Zeng, Ying Lin, Jingyan Li, Shaogui Wang*, Guifang Zhang* and Lin An*

Guangdong Key Laboratory for Translational Cancer Research of Chinese Medicine, Joint Laboratory for Translational Cancer Research of Chinese Medicine of the Ministry of Education of the People's Republic of China, International Institute for Translational Chinese Medicine, School of Pharmaceutical Science, Guangzhou University of Chinese Medicine, Guangzhou, Guangdong, China

Ethnopharmacological relevance: Hepatic fibrosis (HF) occurs in response to chronic liver injury and may easily develop into irreversible liver cirrhosis or even liver cancer. *Amydrium hainanense* water extract (AHWE) is a water-soluble component extracted from the Yao medicine *Amydrium hainanense* (H.Li, Y.Shiao & S.L.Tseng) H.Li, which is commonly used for treating inflammatory diseases in folk. Previous evidence suggested that AHWE significantly inhibited hepatic stellate cell activation. However, little is known regarding the therapeutic effect of AHWE in HF and its underlying action mechanism.

Objective: Investigation of the therapeutic effect of AHWE in HF and its underlying mechanism.

Methods: The therapeutic effect of AHWE was tested *in vivo* using an HF mouse model via an intraperitoneal injection of carbon tetrachloride (CCl₄). Histological evaluation of liver injury and fibrosis were tested by H&E staining and Masson's trichrome staining. Serum levels of ALT, AST, collagen type I (Col I), and hydroxyproline (HYP) were measured. The mRNA expression of liver fibrotic and inflammatory genes were tested, and the protein levels of alpha smooth muscle actin (α -SMA) and signal transducers and activators of transcription 3 (STAT3) were analyzed. The *in vitro* experiments were conducted using HSC-T6 and RAW264.7 cell lines.

Results: Treatment with AHWE significantly reversed histopathological liver damage and liver function abnormalities in CCl₄ mouse model. Also, the serum levels of ALT, AST, Col I, and HYP in CCl₄-induced HF mice were improved in AHWE treatment. Further, AHWE showed a remarkable inhibitory effect on the expression of fibrosis markers (*Acta2*, *Col1a1*, and *Col3a1*) and inflammatory factors (*Stat3*, *Tnfa*, *Il6*, and *Il1b*) induced by CCl₄. The results of *in vitro* experiments were consistent with those obtained *in vivo*. In addition, it is shown that STAT3 signaling was involved in the anti-fibrotic effects of AHWE as evidenced by STAT3 overexpression.

Conclusion: The present study proposed a novel ethnomedicine for HF and suggested the underlying role of STAT3 signaling pathway regulation in this anti-fibrotic effect of the proposed medicine. These findings would serve as solid scientific evidence in support of the development of AHWE as a novel alternative or complementary therapy for HF prevention and treatment.

KEYWORDS

hepatic fibrosis, *Amydrium hainanense*, stat3, α -SMA, carbon tetrachloride

1 Introduction

Hepatic fibrosis (HF) is a reversible and complex wound-healing event secondary to various inflammations and chronic liver injuries (Trautwein et al., 2015). The main characteristic of HF is the excessive extracellular matrix (ECM). When tissue repair occurs in the body, fibrous scars progressively replace the liver parenchyma and distort the vascular architecture of the liver, eventually leading to organ dysfunction (Trautwein et al., 2015). The pathogenic mechanisms of HF may be triggered by several risk factors, such as virus infection, non-alcoholic steatohepatitis (NASH), toxin-related stimuli (e.g., alcohol and chemical), and autoimmune disorders (Parola and Pinzani, 2019). Such damage to liver parenchyma stimulates hepatocytes, Kupffer cells, T cells, and other cells, thereby inducing an inflammatory response, which causes the hepatic stellate cells (HSCs) to transform from a quiescent vitamin A-storing cell lineage to activated myofibroblast-like cells that exhibit contractile properties (Tsuchida and Friedman, 2017). This activation and transformation of HSCs result in the continuous accumulation of alpha-smooth muscle actin (α -SMA), type I and type III collagen (Col I, Col III), and huge amounts of ECM, causing the wound healing response to become pathogenic (Tsuchida and Friedman, 2017). The end-stage of progressive HF is cirrhosis, which has mortal complications. Liver transplantation is the only effective curative therapy available so far (Trautwein et al., 2015). Fortunately, HF is a reversible process, which allows for preventing the progression of fibrosis and reversing advanced HF to inhibit the further progression of hepatopathy, which ultimately reduces mortality. Therefore, it is imperative to explore and discover effective and safe anti-fibrotic drugs.

The currently known mechanisms of HF are based on HSCs, which are resident mesenchymal cells that could serve as the key cells when exploring and designing novel drug targets for HF. In the injured/inflamed hepatic tissue microenvironment, paracrine signals, such as transforming growth factor β (TGF- β), platelet-derived growth factor (PDGF), connective tissue growth factor (CTGF), and other growth factors, may directly or indirectly induce the transdifferentiation of HSCs into matrix protein-secreting myofibroblasts, which subsequently contribute to the excessive deposition of huge amounts of ECM components, particularly Col I and Col III (Barrientos et al., 2008). The

ECM components accumulate in the space of Disse and form fibrous scars, which leads to sinusoidal capillarization characterized by the loss of endothelial fenestrations, ultimately distorting the normal hepatic architecture (Villesen et al., 2020).

The signal transducers and activators of transcription 3 (STAT3) signaling pathway is associated closely with inflammation and regulates the cytokine signaling cascade (Hillmer et al., 2016). STAT3 plays decisive and context-dependent roles in inflammation, tissue survival, and carcinogenesis (Hillmer et al., 2016). A dysregulated or constitutive activation of STAT3 may lead to adverse functional effects, such as impaired immunity and the development of inflammatory diseases and cancers (Yu et al., 2009). Phosphorylated STAT3 forms homodimers, which translocate to the nucleus, thereby allowing an exchange of signals between the cytoplasm and the nucleus. Upon translocation into the nucleus, p-STAT3 forms a complex with certain coactivators, including p68, and binds to the promoter region of target genes for transcription activation. This signaling pathway is reported to be directly involved in the activation and transdifferentiation of HSCs and the subsequent formation of HF (Xiang et al., 2018). The blockade of the STAT3 signaling pathway has been demonstrated to impede the morphological transdifferentiation of HSCs and reduce the mRNA expression of profibrotic genes (Wang et al., 2018).

Amydrium hainanense (H.Li, Y.Shiao & S.L.Tseng) H.Li (AH) is a botanical drug, which is popularly known as China's unique climbing Fujimoto. The AH plant is recognized as folk medicine and functional food in the Yao region. AH has been traditionally used by the Yao people to prevent or cure various human diseases, particularly hepatitis diseases. Moreover, according to ancient records, AH is effective in the treatment of other types of inflammatory diseases, such as hepatitis, gastritis, gastric ulcer, osteomyelitis, cholecystitis, vasculitis, cellulitis, scabies, and rheumatic arthralgia. Therefore, it was speculated that AH would be effective in the treatment of hepatitis owing to its anti-inflammatory activity. A pre-experiment conducted by our research group revealed that the water extract of AH (AHWE) exhibited anti-fibrogenic effects in mice with liver injury. However, the role of AHWE in liver fibrosis and its underlying mechanism remained to be elucidated.

Therefore, the present study aimed to evaluate the potential influence of AHWE on metabolic parameters, liver function, and the pathology of changes in the liver in the experimentally-induced HF model, and subsequently elucidate the possible molecular mechanisms underlying this effect. The study was particularly focused on demonstrating the ability of AHWE to suppress the activation of HSCs and increase the anti-inflammatory response against HF.

2 Materials and methods

2.1 Chemicals and substances

The botanical drugs used in the experiment were collected from Yangshan County, Qingyuan City, Guangdong Province, and were identified as the whole plant of *Amydrium hainanense* (H.Li, Y.Shiao & S.L.Tseng) H.Li by Zhang Guifang, Associate Professor, Guangzhou University of Traditional Chinese Medicine.

Carbon tetrachloride (C11605036) was purchased from Macklin (Shanghai, China). The enhanced BCA protein assay kit (P0010) and the RIPA lysis buffer (P0013) were purchased from the Beyotime Institute of Biotechnology (Shanghai, China). The primary antibodies, namely, the anti-rabbit α -SMA (14395-1-AP), anti-GAPDH (6004-1-Ig), and mouse anti-STAT3 (10253-2-AP), the HEK293-derived recombinant human TGF- β 1 (100-21), and the HRP-labeled AffiniPure goat anti-mouse IgG antibody (H + L) (SA00001-1), were purchased from ProteinTech Group Inc. (Rosemont, IL, United States). The primary antibody rabbit anti-phospho-STAT3 (Tyr705) was purchased from Cell Signaling Technology (Danvers, MA, United States). The HRP-labeled goat anti-rabbit IgG antibody (H + L) (BS13278) was purchased from Bioworld Technology (St. Paul, MN, United States). The Alexa fluor 568-conjugated goat anti-rabbit IgG (H + L) antibody was purchased from Abcam (Cambridge, MA, United States). The Alanine transaminase (Kaiser et al., 2005) assay kit (C009-2-1), the aspartate aminotransferase (AST) assay kit (C010-2-1), and the hydroxyproline examination kit (A030-2-1) were purchased from Nanjing Jiancheng Bioengineering Institute (Nanjing, China). The enzyme-linked immunosorbent assay (ELISA) kit Col-I (E-EL-M 0325c) was purchased from Elabscience (Wuhan, China). The primers used in the real-time PCR analysis were obtained from Sangon Biotech (Shanghai, China). The reagents for western blotting were purchased from Bio-Rad (California Hercules, United States). All chemicals and materials used in the experiments were of analytical grade and obtained from local suppliers.

2.2 Extraction of *Amydrium hainanense* water extract (AHWE)

The dried whole plant of *Amydrium hainanense* was pre-soaked in a 20-fold volume of distilled water and then subjected to extraction for 1 h each time using the water decocting method. Re-extraction was performed two times using the same method, followed by combining all obtained extracts and subjecting the final extract to vacuum filtration. After filtration, the excess solvent was evaporated under reduced pressure using a rotavapor to obtain the crude extract. The crude extract was lyophilized to obtain a fine powder, which was considered the final AHWE and was stored at 4 °C until used in experiments.

2.3 Analysis of the chemical composition of AHWE using the Q-orbitrap technique

Q-Orbitrap is one of the most recently developed mass spectrometry technologies, which is characterized by high resolution and accurate qualitative determination based on multi-level mass spectrometry data. This analytical method is efficient in the rapid identification of complex components in Chinese herbal medicines (Xie and Chen, 2021) (Dong et al., 2020). In the present study, the Q-Orbitrap high-resolution mass spectrometer was used in the Full MS scan/dd-MS2 (Top N) scan mode to accurately determine the mass number and fragment ion acquisition of the samples. The detection instruments used included Thermo Scientific™, Ultimate™3000RS, Thermo Scientific™, Q Exactive™, ESI source, and the RP-C18 column (150 × 2.1 mm, 1.8 μ m). The mass spectrometry conditions were as follows: scan range, 150–2000 m/z; aux gas heater temperature, 350°C; capillary temperature, 300°C; spray voltage, 3.8 kV; and sheath gas pressure, 40 Arb. High purity nitrogen gas (purity \geq 99:999%) was used as both aux gas and sheath gas. High purity argon gas (purity \geq 99:999%) was used as the collision gas. Full-mass and dd-MS2 data in positive and negative modes were obtained at 70,000 and 17,500 FWHM (full width, half maximum), respectively. The chromatography conditions were as follows: column temperature, 35°C; water phase A), 0.1% aqueous solution of formic acid; organic phase B), acetonitrile solution containing 0.1% formic acid. The elution procedure [A:B (v/v) at time (Villesen et al.)] was as follows: (98:2) at 0 min; (98:2) at 1 min; (80:20) at 5 min; (50:50) at 10 min; (20:80) at 15 min; (5:95) at 20 min; (5:95) at 25 min; (98:2) at 26 min; and (98:2) at 30 min. The sample volume injected was 5.00 μ L, and the sample flow rate was 0.30 ml/min. All data were acquired and processed using the CD2.1 software (ThermoFisher), followed by retrieval and comparison in the mzCloud, mzVault, and ChemSpider databases.

2.4 Animals and experimental procedures

Eight-week-old male C57BL/6 mice (body weight 20 ± 2 g) were procured from the Laboratory Animal Center of Guangzhou University of Chinese Medicine [SCXK (Guangdong) 2019–0202]. All experimental procedures were conducted in accordance with the Guiding Principles for the Care and Use of Animals (China) and were approved by the Laboratory Animal Ethics Committee of Guangzhou University of Chinese Medicine (No. ZYD-2020–135) on 12 December 2020.

The mice were acclimatized to the temperature-controlled environment ($22 \pm 2^\circ\text{C}$) and standard 12-h light/12-h dark photoperiod while having free access to food and water. Subsequently, all mice were randomly assigned to the following five groups ($n = 8$): the control group, the CCl_4 group, the low-dose AHWE group (40 mg/kg), the moderate-dose AHWE group (80 mg/kg), and the high-dose AHWE group (160 mg/kg). Liver fibrosis was induced in mice *via* an intraperitoneal (i.p.) injection of 20% CCl_4 [at 1:4 dilution level in olive oil (v/v); dosage: 5 ml/kg body weight] administered twice a week for 4 weeks. The control group mice were administered an i.p. injection of the same volume of olive oil. At the beginning of modeling, all treatment groups received an intragastric administration of AHWE (dissolved in PBS) at the doses of 40, 80, and 160 mg/kg once each day for 4 weeks. On the same day, mice in the control and CCl_4 groups received equal volumes of PBS using a gastric gavage.

After the experimental period, all mice were subjected to a 12-h fasting period, which was followed by euthanization using 1% pentobarbital sodium (i.p. 50 mg/kg) and retrieval of the liver samples. Next, the liver index was calculated using the formula: the liver index = mice liver weight/mice weight $\times 100\%$. The liver lobe was fixed in 4% paraformaldehyde for histological evaluation, while the other liver portions were stored at -80°C until used for further examination.

2.5 Serum biochemical assays

The blood samples were left undisturbed at room temperature for 1 h, followed by centrifugation at 3,000 rpm for 15 min at 4°C . The obtained sera were subjected to the evaluation of alanine aminotransferase (Kaiser et al., 2005) and aspartate aminotransferase (AST) levels using the protocols provided in the respective kits.

2.6 Enzyme-linked immunosorbent assay (ELISA)

The liver tissue samples were homogenized in PBS, on ice, followed by centrifugation at 5,000 g for 10 min at 4°C . The

obtained tissue supernatant was subjected to the evaluation of the expression of inflammatory indicators, including Tnfa, Il1 β , and Il6, using ELISA kits following the specific instructions provided by the manufacturer.

2.7 Liver histopathology and immunohistochemical examination

In order to assess morphological changes in the liver tissue, the liver tissues were treated with 4% paraformaldehyde and embedded in paraffin. Subsequently, 5 μm sections were excised from the paraffin blocks and mounted on slides. The paraffin-embedded tissue samples were stained with the hematoxylin and eosin (H&E) stain for histopathological examination or with Masson's trichrome stain for collagen level determination. The stained sample slides were examined under a digital scanner (E100, Nikon Corporation). Meanwhile, the paraffin-embedded tissues for all groups were subjected to immunohistochemical staining for STAT3 and visualized using a section digital scanner (E100, Nikon Corporation).

2.8 Cell culture and AHWE treatment

The rat hepatic stellate cell line T6 (HSC-T6) was kindly provided by the Zhejiang Cancer Hospital (Zhejiang, China). The cells were cultured in Dulbecco's modified Eagle's medium (DMEM, Thermo Fisher Scientific, MA, United States) supplemented with 10% fetal bovine serum (FBS, Thermo Fisher Scientific, MA, United States), 100 U/mL of streptomycin, and 100 U/mL of penicillin at 37°C inside a humidified incubator with 5% CO_2 and 95% air. Upon reaching the desired confluence, the cells were washed two times with PBS and cultured in a fresh serum-free medium prior to subsequent experiments.

In order to establish the HSCs injury model, the HSC-T6 cells were treated with 10 ng/ml of transforming growth factor beta 1 (TGF- β 1) for 1 h for stimulation. Subsequently, AHWE was added directly at different doses (0.25, 0.5, and 1 mg/ml) to the DMEM supernatant containing TGF- β 1, followed by 24 h of incubation. The inflammatory cell model was established by treating the RAW264.7 cell line with 1 $\mu\text{g}/\text{ml}$ of lipopolysaccharide (LPS) for 1 h. Afterward, the drug solution was added directly at different doses (0.25, 0.5, and 1 mg/ml) to the DMEM supernatant containing LPS, followed by 24 h of incubation.

2.9 Cell viability assay

Cellular viability was evaluated using the CCK-8 assay kit (GLPBIO, California, United States). The HSC-T6 cells were cultured in 96-well culture plates and then treated with different concentrations of AHWE ranging from 0 to 2.5 mg/ml for 24 h.

TABLE 1 Sequences of primers used for RT-qPCR.

Species	Primers	Sequences
<i>Mus musculus</i>	<i>Gapdh</i> -forward	GCCTCGTCCCGTAGACAAAA
	<i>Gapdh</i> -reverse	TACGGCCAAATCCGTTCCACA
	<i>Acta2</i> -forward	GAAGCTCGTTATAGAAAAG AGTGG
	<i>Acta2</i> -reverse	TCAGGGAGTAATGGTTGGAAT
	<i>Col1a1</i> -forward	TTCTCCTGGCAAAGACGGAC
	<i>Col1a1</i> -reverse	CGGCCACCATCTTGAGACTT
	<i>Col3a1</i> -forward	ACGTAAGCACTGGTGGACAG
	<i>Col3a1</i> -reverse	CAGGAGGGCCATAGCTGAAC
	<i>Il1β</i> -forward	TGCCACCTTTTGACAGTGATG
	<i>Il1β</i> -reverse	TGATGTGCTGCTGCGAGATT
	<i>Il6</i> -forward	GTCCTTCCTACCCCAATTCCA
	<i>Il6</i> -reverse	CGCACTAGGTTTGGCCGAGTA
	<i>Tnfa</i> -forward	ATGGCTCCCTCTCATCAGT
	<i>Tnfa</i> -reverse	TTTGCTACGACGTGGGCTAC
<i>Stat3</i> -forward	TGTCAGATCACATGGGCTAAAT	
<i>Stat3</i> -reverse	GGTCGATGATATTGTCTAGCCA	
<i>Rattus norvegicus</i>	<i>Gapdh</i> -Forward	AGTGCCAGCCTCGTCTCATA
	<i>Gapdh</i> -Reverse	GATGGTGATGGGTTTCCCGT
	<i>Acta2</i> -forward	CATCCGACCTTGCTAACGGA
	<i>Acta2</i> -reverse	GTCCAGAGCGACATAGCACA
	<i>Col1a1</i> -forward	GTGCGATGGCGTGCTATG
	<i>Col1a1</i> -reverse	ACTTCTGCGTCTGGTGATAACA
	<i>Col3a1</i> -forward	AGATGCTGGTGCTGAGAA GAAAC
	<i>Col3a1</i> -reverse	GCTGGAAAGAAGTCTGAG GAAGG

Next, the CCK-8 solution (10 μ L) was added to each well, and the absorbance was measured after 1 h of incubation using a microplate reader (Thermo Varioskan LUX, MA, United States) at 450 nm. Each experiment was conducted in triplicate for each group. Percent viability was calculated as the absorbance of the cells treated with different doses of AHWE relative to that of the control cells.

2.10 Immunofluorescence staining

RAW264.7 cells cultured on confocal dishes were treated with the corresponding stimuli. After washing with PBS, the cells were treated with 4% paraformaldehyde for 15 min at room

temperature for fixing and then permeabilized with PBS containing 0.1% Triton X-100 for another 10 min at room temperature. Next, the cells were blocked by exposure to 10% goat serum for 30 min at room temperature, followed by overnight incubation at 4°C with the mouse antibody against STAT3 (for STAT3 subcellular detection) in 10% goat serum. After the incubation, the dishes were washed and incubated with Alexa Fluor 594-conjugated secondary antibody in the dark at room temperature for 1 h. The nuclei were detected through 10 min of staining with the DAPI solution in the dark at room temperature. Finally, the dishes were washed and then visualized and photographed under a Zeiss LSM 510 laser confocal fluorescence microscope (Carl Zeiss, Oberkochen, Germany).

2.11 Quantitative real-time polymerase chain reaction (RT-qPCR)

Total RNA was extracted from cells or liver tissues using Trizol Reagent (Accurate Biotechnology, Human, China) according to the manufacturer's instructions. The purity and concentration of the extracted RNA sample were measured using NanoDrop 2000 spectrophotometer from ThermoFisher Scientific (Waltham, MA, United States). Subsequently, 1 ng of the extracted total RNA was used for synthesizing cDNA using the *Evo M-MLV* RT kit, and the gDNA Clean was used for conducting RT-qPCR (Accurate Biotechnology, Human, China). The RT-qPCR experiment was conducted in triplicate for each cDNA sample using the SYBR Green Premix *Pro Taq* HS qPCR kit (Accurate Biotechnology, Human, China) and the gene-specific primer pairs for *Gapdh*, *Col1a1*, *Col3a1*, *Il1β*, *Il6*, *Tnfa*, and *Acta2*. A QuantStudio five Real-Time PCR instrument (ThermoFisher Scientific, MA, United States) was employed for PCR amplification under the following reaction conditions: 40 cycles of enzyme activation at 95°C for 30 s, denaturation at 95°C for 5 s, and annealing and extending at 60°C for 30 s. The primer sequences used are presented in Table 1. The mRNA expression was calculated using the $2^{-\Delta\Delta CT}$ method and GAPDH as the internal control.

2.12 Plasmid transfection

The STAT3 plasmid was constructed using pEGFP-N3. The plasmid construction was confirmed through DNA sequencing, which was conducted in Sangon Biotech Co. Ltd. (Shanghai, China). The constructed plasmid was then transiently transfected into HSC-T6 and RAW264.7 cells using Lipofectamine 2000 reagent (Invitrogen, Carlsbad, CA, United States) according to the manufacturer's instructions. After 24 h, the cells were cultured in a fresh medium and used for subsequent experiments.

2.13 Western blotting analysis

The liver tissue and cultured cell lysates were prepared, on ice, using RIPA lysis buffer containing a protease inhibitor cocktail. The concentration of proteins in the lysates was determined using the BCA protein assay kit (Pierce, United States). Equal amounts of proteins were separated using 10%~12% sodium dodecyl sulfate-polyacrylamide gel electrophoresis (SDS-PAGE) run at 55 V for 30 min and then at 120 V for 60 min. The separated proteins were transferred from the gels to methanol-pres soaked polyvinylidene fluoride (PVDF) membranes under the action of a constant current of 350 A for 70 min. Next, the membranes were blocked using 5% skimmed milk (FUJIFILM Wako Pure Chemical Corporation, Fuji, Japan), followed by incubation at room temperature for 2 h and subsequent washing with Tris-buffered saline Tween (TBST). The membranes were then incubated overnight at 4°C with primary antibodies against GAPDH, α -SMA, and STAT3 (used at 1:1000 dilution), followed by incubation with the appropriate horseradish peroxidase-conjugated secondary antibody against rabbit or mouse IgG (used at 1:10000 dilution). The band intensities were developed using ECL enhanced chemiluminescence (Yeasen, Shanghai, China) and quantified using Image-ProPlus 6.0 software (Rockville, MD, United States).

2.14 Statistical analysis

All experiments were randomized and blinded. The result data were expressed as the mean \pm SD (standard deviation) of a minimum of three independent experiments. The result data were analyzed statistically by performing Dunnett's test and one-way ANOVA using GraphPad Prism version 7.0 (San Diego, CA, United States). The statistical significance threshold was set at $p < 0.05$.

3 Results

3.1 Chemical composition of AHWE

The phytochemical compounds present in AHWE were isolated and characterized using the Q-Orbitrap technique. CD2.1 (Thermo Fisher) was employed to preliminarily organize the collected high-resolution liquid quality data, which was followed by searching the databases mzCloud, mzVault, ChemSpider for data comparison. The database search revealed 10 compounds with the mzCloud score of 80 or higher. The total ion chromatogram of AHWE is depicted in Figure 1. The characterization results for the compounds (salsolinol, α -eleostearic acid, corchori fatty acid

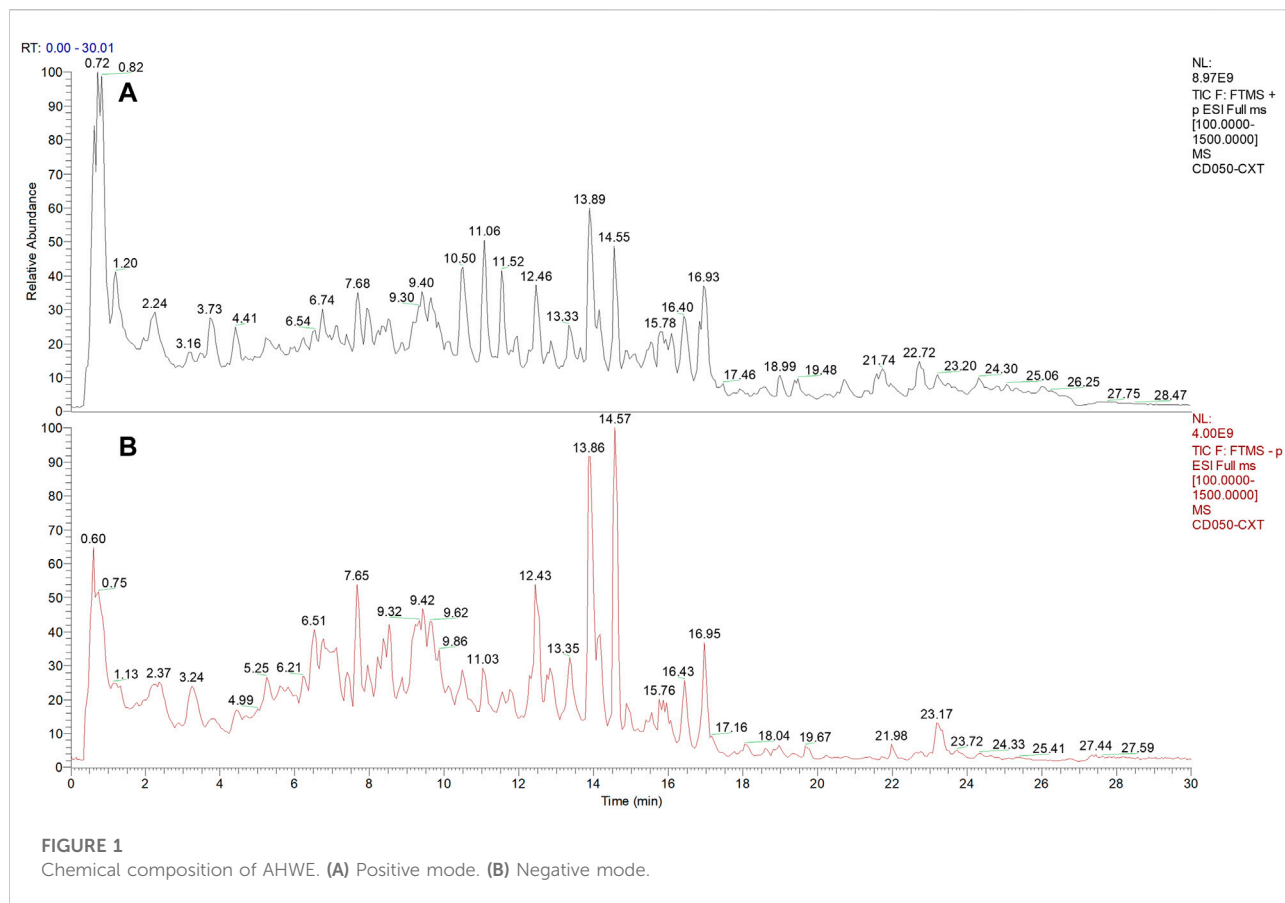
F, 1-phenylalanine, trans-3-Indoleacrylic acid, 9-oxo-10E), 12 (E)-octadecadienoic acid, (+/-)12 (13)-DiHOME, (-)-caryophyllene oxide, citric acid, and trans-4-indoleacrylic acid) are presented in Table 2.

3.2 AHWE improved the CCl₄-induced pathological damage in the liver of HF mice

In order to evaluate the effects of AHWE on the CCl₄-induced HF in mice, the body weight, liver weight, liver index, hepatic histopathological changes, and plasma markers of these mice were monitored (Figure 2). As depicted in Figure 2A, the control group mice exhibited progressive weight gain compared to the CCl₄ group. In the AHWE-treated mice, no significant difference was observed in the body weight, and the liver weight and liver coefficient values were rescued (Figures 2B, C). Moreover, the morphological changes in the dissected liver samples caused due to CCl₄ administration were notably improved upon AHWE administration (Figure 2D). These findings were confirmed in the H&E staining results. The H&E stained liver tissue samples from the control group revealed normal hepatocytes with a prominent nucleolus and a complete cytoplasmic pattern and structure of liver lobules. On the contrary, the samples from the CCl₄ administration group exhibited damaged hepatocytes, inflammatory cell infiltration, necrosis, and steatosis, in addition to visible fat vacuoles. However, these pathological changes in the CCl₄ group mice were evidently improved in the liver samples from the AHWE-treated mice (Figure 2E). AST and ALT are considered important markers of CCl₄ hepatotoxicity. In the present study, it was revealed that CCl₄ administration significantly elevated the levels of ALT and AST (Figures 2F, G). After treatment with AHWE, the liver function of mice demonstrated a trend of recovery. Collectively, the above results suggested that AHWE attenuated the CCl₄-induced liver pathological damage. Accordingly, based on the hepatoprotective effects of AHWE, it was speculated that AHWE possibly contributes to the prevention of liver fibrosis.

3.3 AHWE exhibited an anti-fibrotic effect in CCl₄-induced HF mice

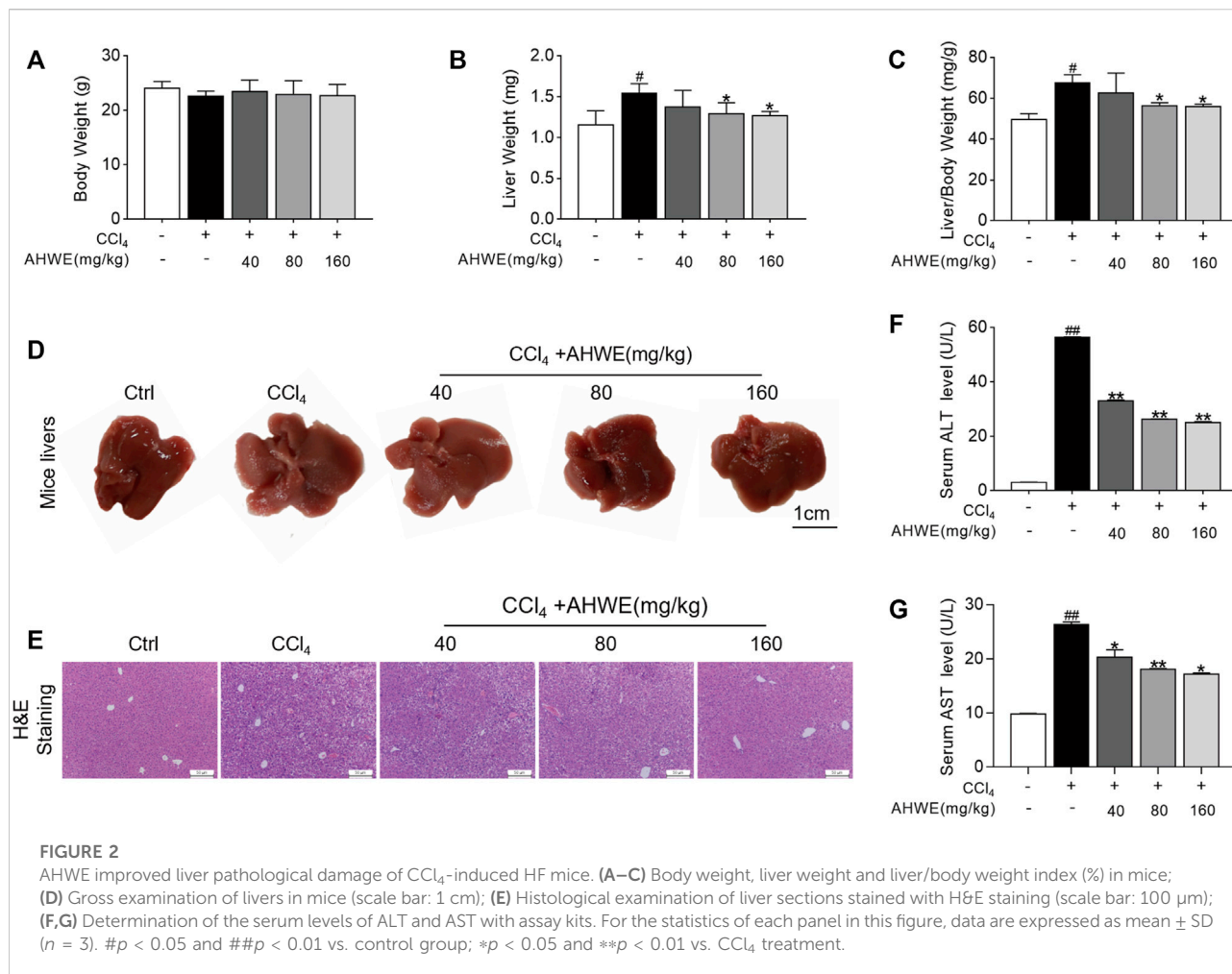
In order to further evaluate the potential of AHWE in reducing liver fibrosis, Masson's trichrome staining was performed. According to the staining results, AHWE treatment dramatically mitigated collagen deposition, connective tissue hyperplasia, and pseudo-lobule formation induced by CCl₄ administration (Figure 3A, left panel). The fibrosis indicated in blue in Masson sections was semi-

**TABLE 2** Identification of the chemical constituents in AHWE.

NO.	m/z	RT Villesen et al. (2020)	Formula	Peak area	Identification
1	162.0677	0.673	C ₁₀ H ₁₃ NO ₂	292352457	Salsolinol
2	278.2234	16.994	C ₁₈ H ₃₀ O ₂	284337100	α-Eleostearic acid
3	328.2246	13.357	C ₁₈ H ₃₂ O ₅	205948422	Corchorifatty acid F
4	148.0523	1.197	C ₉ H ₁₁ NO ₂	126521147	L-Phenylalanine
5	187.0631	2.266	C ₁₁ H ₉ NO ₂	124378283	trans-3-Indoleacrylic acid
6	294.2186	13.924	C ₁₈ H ₃₀ O ₃	112510287	9-Oxo-10(E),12(E)-octadecadienoic acid
7	314.2452	15.999	C ₁₈ H ₃₄ O ₄	108470966	(+/-)-12 (13)-DiHOME
8	220.182	12.501	C ₁₅ H ₂₄ O	103084519	(-)-Caryophyllene oxide
9	192.0263	0.742	C ₆ H ₈ O ₇	82592598	Citric acid
10	278.1512	16.094	C ₁₆ H ₂₂ O ₄	34670922	trans-4-Indoleacrylic acid

quantified (Figure 3A, right panel). Consistent with these observations, the ELISA results in the present study revealed that AHWE reduced the levels of Col I in CCl₄-induced HF mice (Figure 3B). Similar results were observed in the detection

of hydroxyproline (HYP), a major component of all types of fibrillar collagen (Figure 3C). Alpha smooth muscle actin (α-SMA) is considered a marker of the activation of HSCs in the pathological process of HF (Tarbit et al., 2019). The quantified



result data from the western blot analysis conducted in the present study revealed that CCl₄ administration increased the expression of α -SMA in livers, while the treatment with AHWE inhibited the expression of this protein in CCl₄-induced HF mice (Figure 3D). In addition, fibrotic genes, such as *Acta2*, *Col1a1*, and *Col3a1*, were analyzed using RT-qPCR, which revealed an evident increase in the mRNA levels of all three genes in the CCl₄ group compared to the control group. However, in the AHWE treatment groups, these levels were markedly downregulated compared to the CCl₄ group (Figure 3E). Considering the crucial role of inflammation in HF, the levels of common inflammatory factors, such as *Tnfa*, *Il6*, and *Il1 β* , were evaluated. It was observed that compared to the control group, the CCl₄ group exhibited elevated mRNA expression levels of cytokines, while this effect was abolished after AHWE treatment (Figure 3F). These observations confirmed the anti-fibrotic effect of AHWE in CCl₄-induced HF mice and that AHWE could suppress the inflammatory response during liver fibrosis.

3.4 AHWE inhibited hepatic stellate cell activation and suppressed inflammation in cellular experiments

Inspired by the findings of *in vivo* experiments, the anti-fibrotic effects of AHWE and the underlying mechanisms were evaluated *in vitro* as well. In these evaluations, HSC-T6 cells and RAW264.7 cells were used. First, the potential cytotoxicity of AHWE in the above 2 cell types was evaluated, and the statistically analyzed results are presented in Figure 4A. As evident, 2.5 mg/ml AHWE significantly affected cell viability in both cell types ($p < 0.05$), while AHWE in the concentration range of 0.005–1.25 mg/ml was almost non-toxic to the 2 cell types (although with no statistically significant difference). Therefore, in the next experiment, three appropriate doses of AHWE (0.25, 0.5, and 1 mg/ml) were tested to exclude the possibility of AHWE being cytotoxic and thereby causing the inhibition of HSC activation and inflammation.

Furthermore, consistent with the *in vivo* results, AHWE downregulated the α -SMA protein levels induced by TGF- β 1

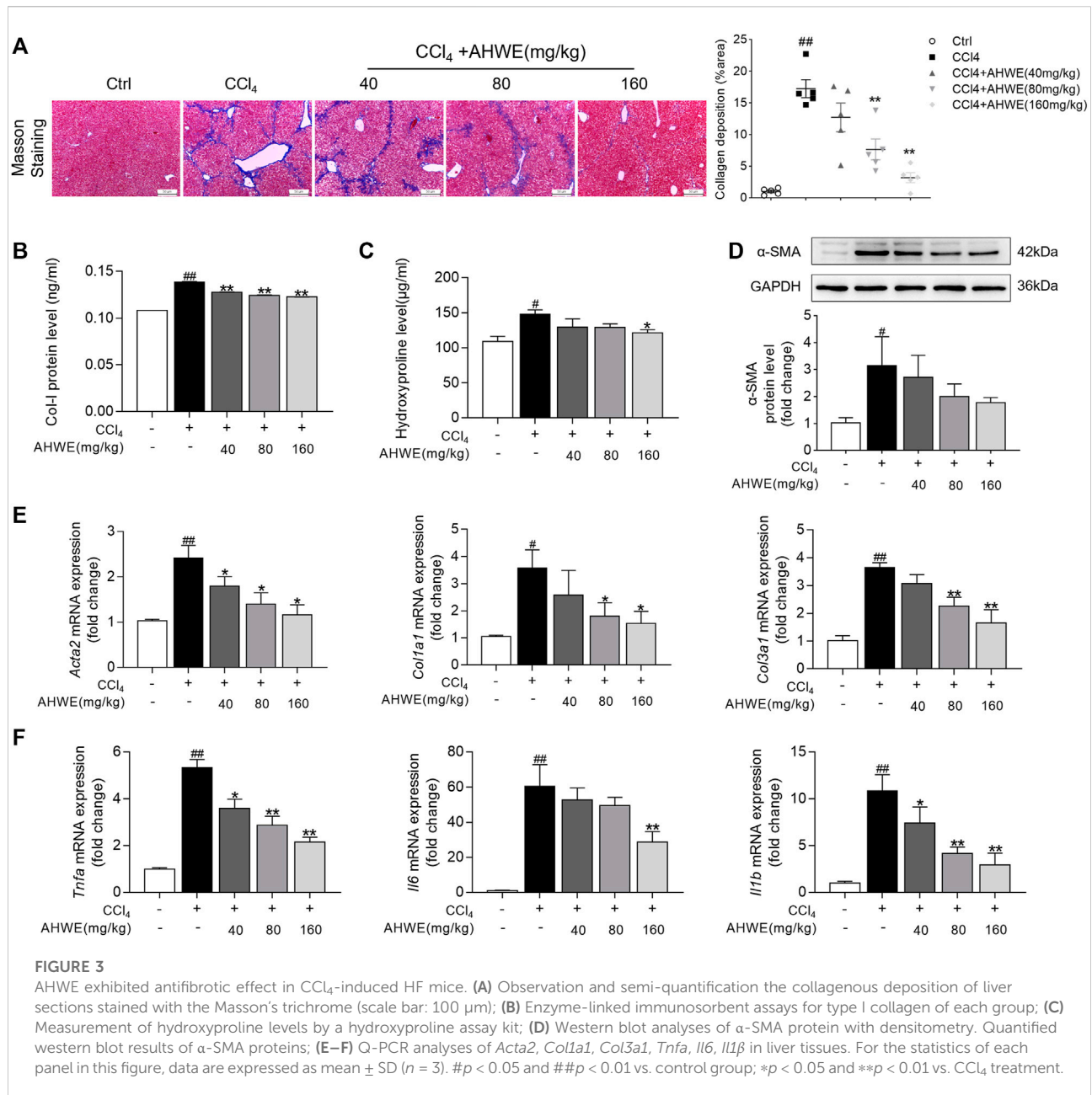
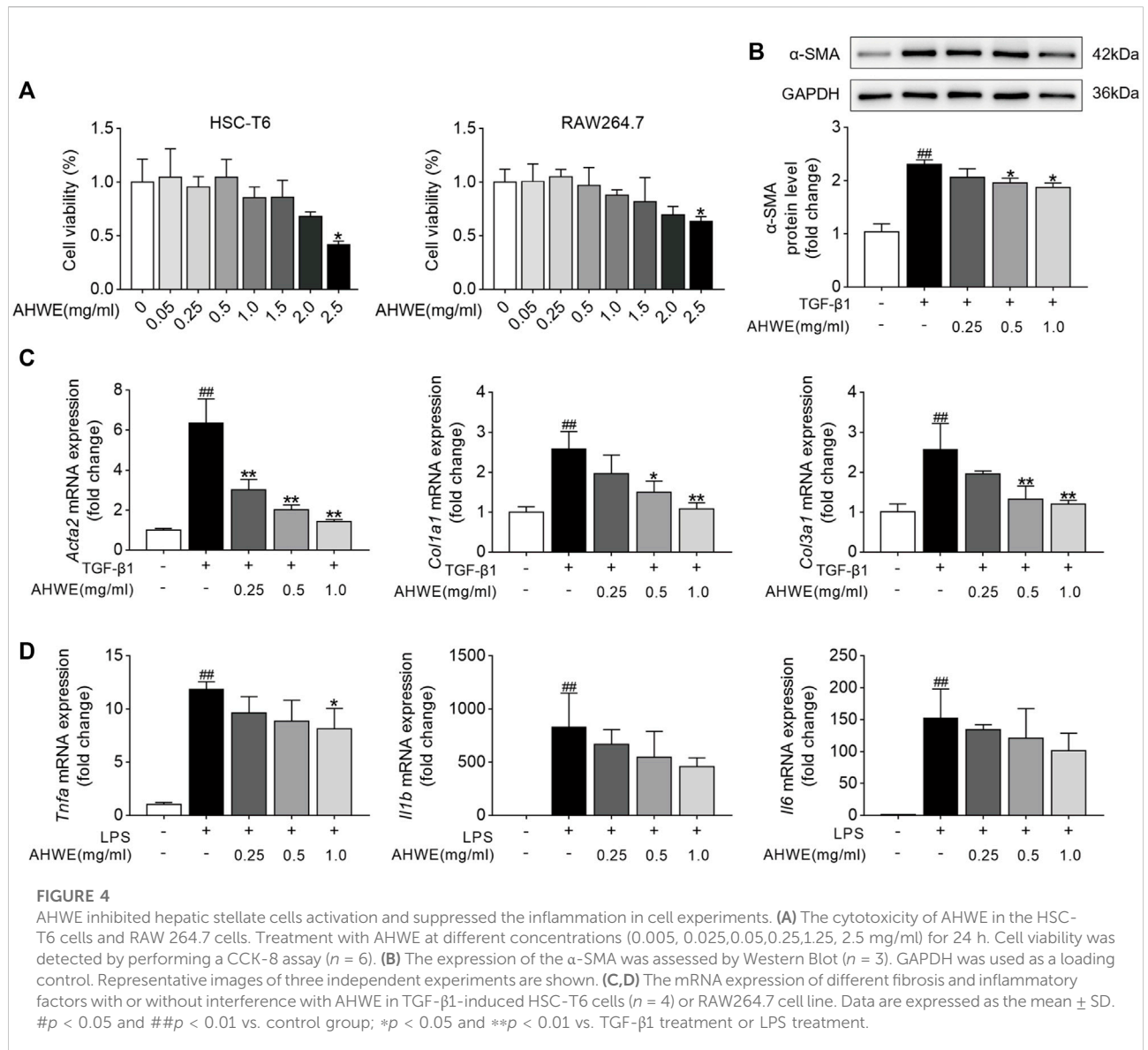


(Figure 4B). In addition, the differentially expressed genes associated with the fibrosis process in HSC-T6 cells, including *Acta2*, *Col1a1*, and *Col3a1*, were identified using the RT-qPCR method. The genes related to the inflammatory process, such as *Tnfa*, *Il6*, and *Il1β*, were also identified using the same method. The results revealed that TGF-β1 stimulation markedly increased the mRNA expression levels of *Acta2*, *Col1a1*, and *Col3a1* in HSC-T6 cells, while LPS stimulation upregulated the mRNA expression levels of *Tnfa*, *Il6*, and *Il1β* in RAW264.7 cells (Figures 4C, D). As expected, these effects were significantly reversed ($p < 0.05$) upon AHWE treatment in a dose-dependent manner

(Figures 4C, D). Collectively, these results suggested that this botanical drug exerted a remarkable inhibitory effect on hepatic stellate cell activation and inflammatory responses.

3.5 STAT3 signaling pathway could be involved in the regulation of the anti-fibrotic responses of AHWE

Inflammation serves as a fuel that accelerates liver cell proliferation and tissue regeneration, thereby playing a pivotal



role in the pathogenesis of liver fibrosis (Tanwar et al., 2020). Accumulating evidence suggests that STAT3 is closely associated with the occurrence and development of liver fibrosis caused by various factors (Xiang et al., 2018) (Wang et al., 2018). Persistent activation of STAT3 exerts a pro-inflammatory effect, which leads to various pathological manifestations in liver fibrosis. In order to explore whether AHWE exerts an effect on STAT3, the protein levels of STAT3 and p-STAT3 in RAW 264.7 cells were determined using western blotting. The blot images and the quantified data, depicted in Figure 5A, revealed that the trend of increase in the p-STAT3 to STAT3 ratio was higher in the LPS stimulation group than in the control group. AHWE decreased the levels of total and phosphorylated STAT3. In addition, the mRNA expression levels of *Stat3* in RAW264.7 cells were determined using the RT-qPCR method, and it was revealed

that the mRNA expression of *Stat3* in the RAW cells stimulated by LPS was significantly increased compared to the control group (Figure 5B). The presence of AHWE relieved this effect in a dose-dependent manner ($p < 0.05$). STAT3 is located mainly in the cytoplasm of resting cells and, in response to activation, translocates to the nucleus to play its role *via* transcriptional regulation. TGF- β 1 was observed to increase the STAT3 expression in the nucleus, while STAT3 protein in the cytoplasm was concordantly reduced, which indicated the translocation of STAT3 to the nucleus (Figure 5C). The confocal microscopy observations confirmed the functional role of AHWE in the inhibition of STAT3 activation (Figure 5C). The above experimental evidence indicated that STAT3 signaling pathway could be involved in the regulation of anti-fibrotic responses.

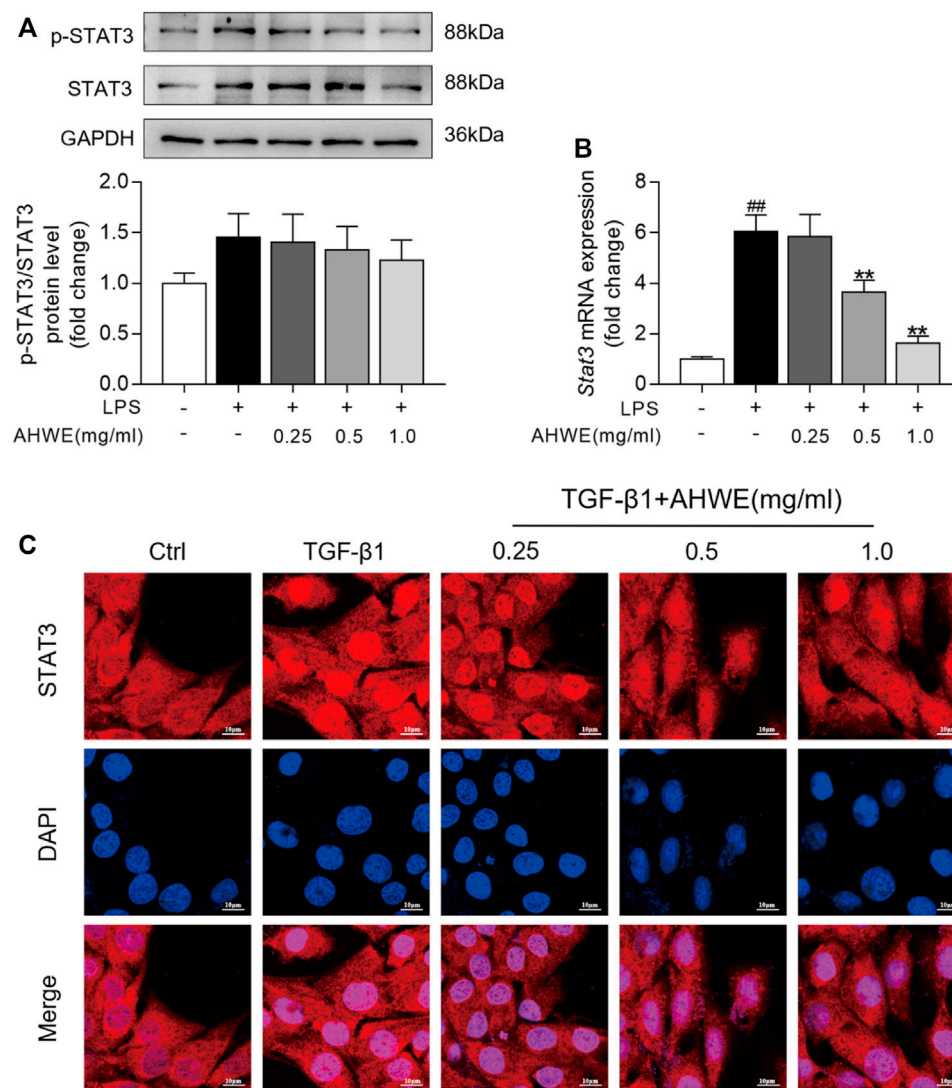


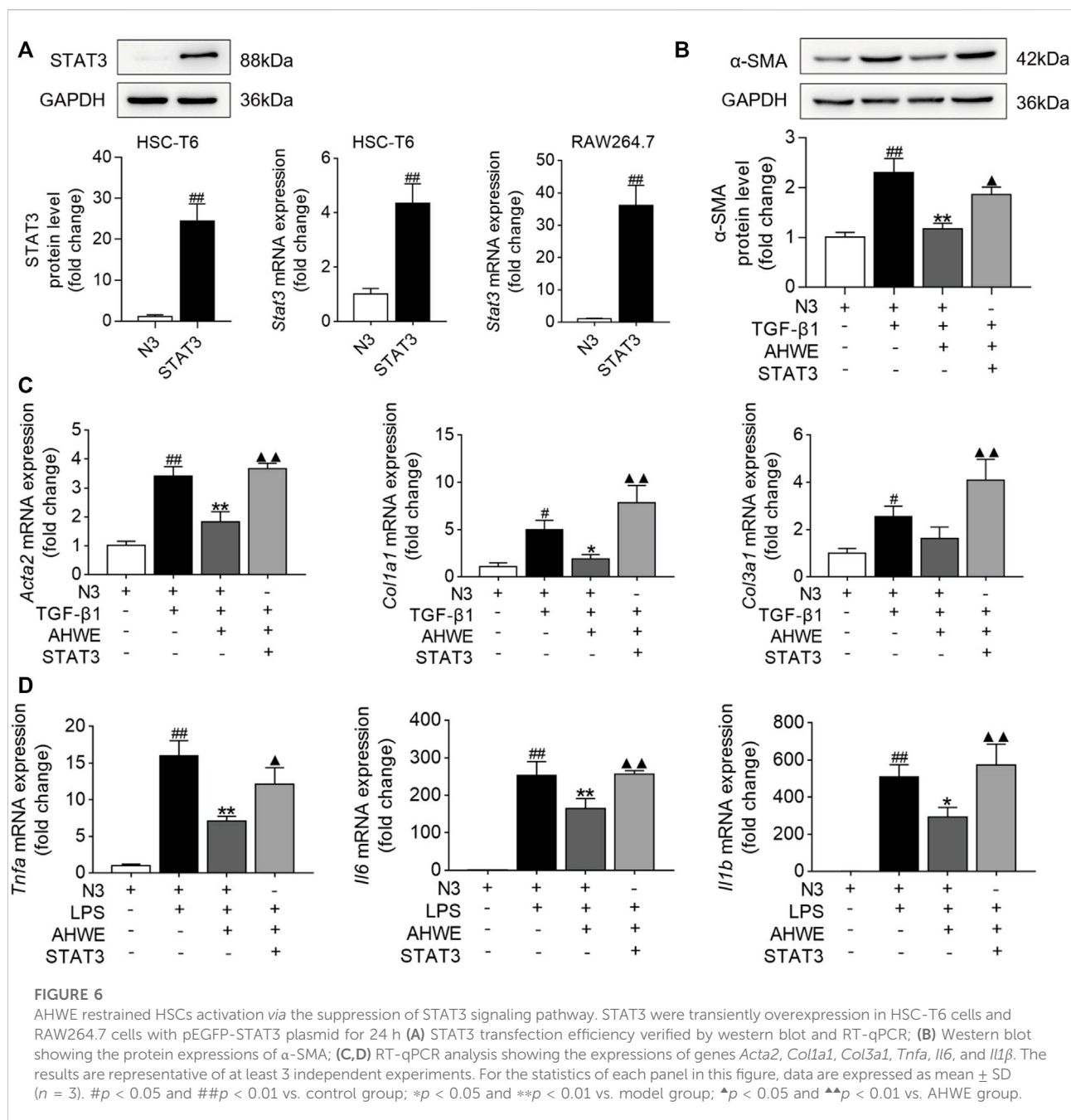
FIGURE 5

STAT3 signaling pathway might be involved into the regulation of antifibrotic responses by AHWE. **(A)** Western Blotting for phosphorylated STAT3 and total STAT3; Densitometric analyses of bands were quantified, and data expressed as fold of control normalized to GAPDH. **(B)** Expression of *Stat3* mRNA was determined by Q-PCR. The results are representative of at least 3 independent experiments. **(C)** Confocal scanning images of STAT3 nucleus trafficking in HSC-T6 cells stimulated with TGF-β1 (10 ng/ml) for 24 h ($n = 3$), scale bar = 10 μm. Data are expressed as mean ± SD ($n = 3$). # $p < 0.05$ and ## $p < 0.01$ vs. control group; * $p < 0.05$ and ** $p < 0.01$ vs. TGF-β1 treatment.

3.6 AHWE restrained HSC cell activation through suppression of the STAT3 signaling pathway

The potential role of the STAT3 signaling pathway in the AHWE regulatory effect on the anti-fibrosis response was further ascertained experimentally using the pEGFP-STAT3 plasmid or the empty N3 vector. The results of western blotting and RT-qPCR verified the successful overexpression of the *Stat3* gene in HSC-T6 cells and RAW264.7 cells. As depicted in Figure 6A,

STAT3 was overexpressed upon STAT3 plasmid transfection. Next, western blotting was performed to evaluate the levels of α-SMA in the HSC-T6 cells transfected with STAT3 plasmid, and the result data were quantified. As depicted in Figure 6B, the expression levels of this important marker protein were significantly increased upon stimulation with TGF-β1 compared to stimulation with the empty N3 vector. This effect was significantly improved upon treatment with AHWE. The protein expression levels of the fibrosis marker α-SMA were also significantly increased upon STAT3 overexpression,

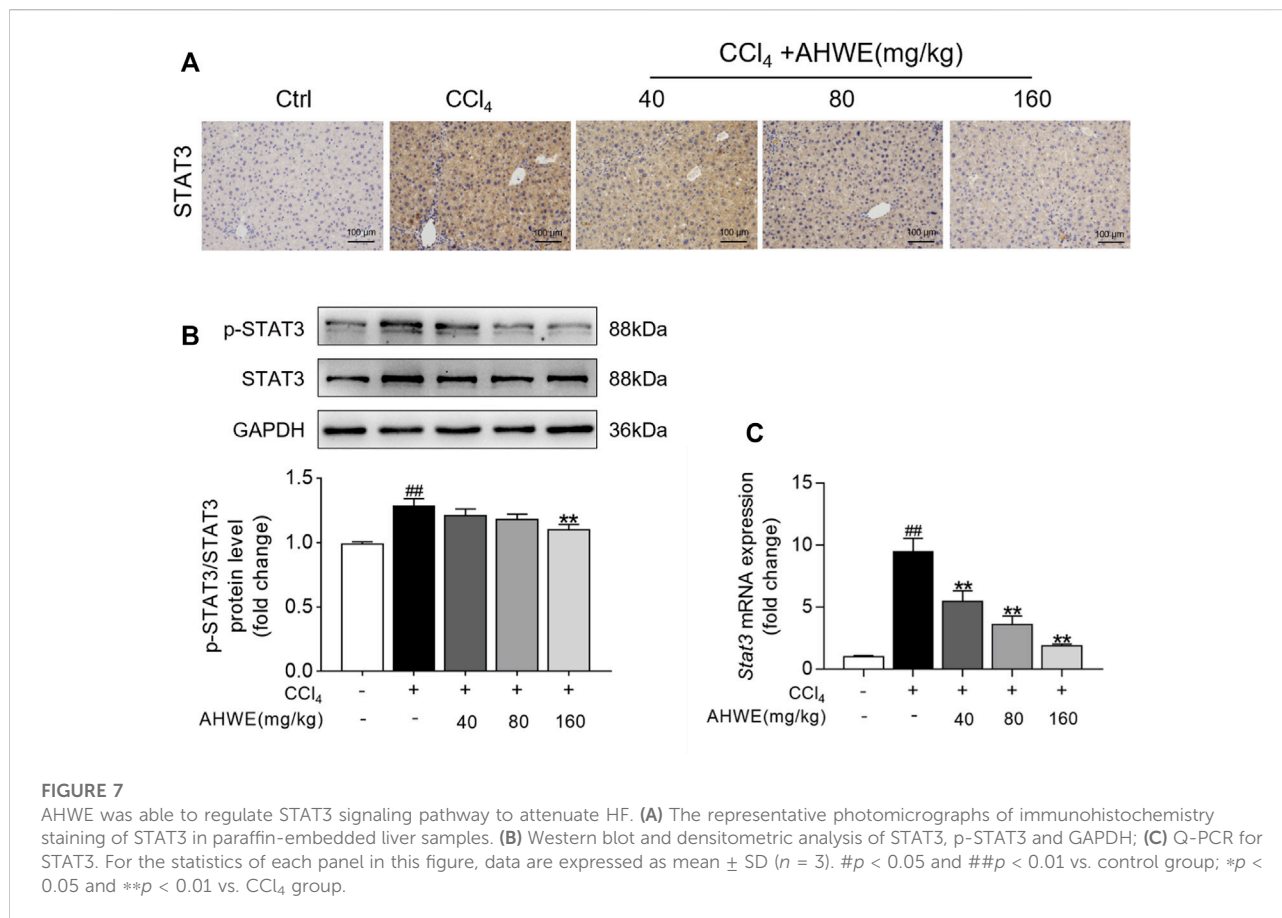


suggesting that STAT3 suppressed the activation of HSCs. In addition, the mRNA expression levels of the fibrosis markers *Acta2*, *Col1a1*, and *Col3a1* and those of the inflammatory markers *Tnfa*, *Il6*, and *Il1 β* in the HSC-T6 cells transfected with the STAT3 plasmid were determined (Figures 6C, D). It was revealed that the effect of downregulation of these genes due to AHWE treatment was significantly reversed upon STAT3 overexpression (Figures 6C, D). These findings further elucidated that the *in vitro* anti-fibrotic

effect of AHWE was indeed mediated by the STAT3 signaling pathway.

3.7 AHWE could regulate the STAT3 signaling pathway to attenuate HF

The above-stated findings of *in vitro* experiments verified that AHWE could restrain the activation of HSCs by inhibiting the



STAT3 signaling pathway. However, the underlying consistent regulatory mechanism in mice was unverified so far. Therefore, STAT3 levels in the liver tissue samples from the mice in each experimental group were examined immunohistochemically. The analysis revealed an up-regulation of STAT3 expression in the CCl₄-induced liver fibrosis tissue samples, while AHWE assisted in reducing this undesirable trend (Figure 7A). Next, the protein levels of STAT3 and p-STAT3 in the liver samples were analyzed using immunoblotting, and the results are presented in Figure 7B. As visible in the figure, the p-STAT3 to STAT3 ratio was higher in the CCl₄-induced HF mice liver tissue relative to the control, while the ratio was decreased upon treatment with AHWE. Furthermore, the expression levels of the *Stat3* gene in the liver samples were determined. A higher expression of STAT3 was detected in the HF tissues compared to the normal liver tissues. In the presence of AHWE, the mRNA expression levels of this gene decreased significantly in a dose-dependent manner (Figure 7C). These results provided evidence in support of the involvement of STAT3 signaling pathway in the *in vivo* suppression of HF upon AHWE treatment. Therefore, it was concluded that AHWE could restrain the activation of HSCs through the suppression of the STAT3 signaling pathway, which ultimately mitigated liver fibrosis.

4 Discussion

HF is characterized by the excessive accumulation of the extracellular matrix or the presence of excessive connective tissue in response to liver inflammation and chronic liver injury (Wynn and Ramalingam, 2012). As HF progresses, it often develops into irreversible cirrhosis or even liver cancer in certain cases, thereby raising a major threat to public health. Activated HSCs, which are capable of transforming into myofibroblast-like cells, are recognized as the effector cells in liver fibrosis (da Silva Meirelles et al., 2020). Therefore, HSCs are considered the main fibrogenic precursor cells in the liver. This activation of HSCs is characterized by the gradual release of intracellular vitamin A, an increased rate of cell proliferation, α -SMA activation, the synthesis of a fibrogenic matrix rich in Col I and Col III, and a higher expression of the extracellular matrix that distorts the liver architecture by forming liver fiber nodules and consequently disrupts the normal functioning of the liver, ultimately causing pathophysiological damage to the organ (Ding et al., 2021). The blockade and/or reversal of this activation of HSCs determines the efficacy of any anti-fibrotic therapy and is, therefore, the key target in HF treatment. The release of pro-inflammatory cytokines from hepatocytes and Kupffer cells is

reported as a critical step in the pathogenesis of HF (Wu et al., 2019). The resulting activation of immune cells, such as monocytes, neutrophils, and lymphocytes, is also important for the development of liver injury (Adams et al., 2010). In the liver, *Tnf- α* , *Il6*, and *Il1 β* may trigger the accumulation of neutrophils and monocytes, thereby contributing to the early stages of disease progression and maintaining persistent inflammation of the liver tissue (Kany et al., 2019).

The mechanisms underlying fibrosis are not completely understood to date, due to which no highly effective therapy is currently available for liver fibrosis. Therefore, it is imperative to explore and develop novel therapies and medicines for treating liver fibrosis. As botanical drugs are gaining increasing attention as sources of novel bioactive substances and have begun replacing synthetic pharmaceuticals, using herbal medicinal in HF treatment appears to be an attractive option as a viable and effective alternative strategy (Latief and Ahmad, 2018). *Amydrium hainanense* (H.Li, Y.Shiao & S.L.Tseng) H.Li is reported to have potential medicinal value in regard to liver diseases, especially liver inflammation. This unique Chinese climbing Fujimoto has been used widely as a folk medicine in the Yao region. A pre-experiment conducted by our research group also confirmed that the water extract of AH could exhibit anti-fibrogenic effects in mice with liver injury.

In this context, the present study pioneered in confirming the therapeutic value of AHWE in HF, both *in vivo* and *in vitro*, in addition to elucidating that this effect of AHWE was mainly based on the suppression of HSC activation and proliferation via STAT3 signaling pathway inhibition. The liver fibrosis model was established using 20% CCl₄. The hepatic pathology analysis based on H&E staining confirmed the successful establishment of typical liver fibrosis in the model group mice. Upon AHWE treatment, improvement in the hepatic lobule structure and reduced inflammatory cell infiltration was observed in a dose-dependent manner. The ALT and AST levels are low under physiological conditions in normal hepatocytes, while large amounts of these enzymes are released into the blood when the hepatocytes are damaged, which results in a sharp increase in the serum activities of ALT and AST (Kim et al., 2020). Therefore, serum ALT and AST levels are two typical and major biochemical parameters marking liver injury. In the present study, the serum activities of ALT and AST exhibited an upward trend in the model group, indicating declining liver function. This undesirable pathological damage to the liver tissue was improved upon AHWE treatment. The liver sections stained using Masson's trichrome stain exhibited hepatic histopathological changes, including damaged lobular structure and excessive fat and collagen deposition in the model mice, and these changes were significantly improved upon AHWE treatment. The various

examinations of different factors associated with liver fibrosis revealed that, compared to the CCl₄ group, the AHWE administration group exhibited decreased levels of Col I, hydroxyproline, and α -SMA protein. Among the well-recognized mediators, TNF- α , IL-6, and Il1 β have been implicated in the regulation of inflammation in liver diseases. TNF- α reportedly induces hepatocyte proliferation, apoptosis, and inflammation, in addition to suppressing Col I gene expression (Yang and Seki, 2015). IL-6 has reportedly presented the strongest correlation with fibrosis severity in biopsy patients (Ridner et al., 2018). The q-PCR analysis results of the present study revealed that the expression levels of *Acta2*, *Col1a1*, *Col3a1*, *Tnfa*, *Il6*, and *Il1 β* in the liver tissue samples were decreased upon treatment with AHWE. These data suggested that AHWE exerted an anti-fibrotic effect on the CCl₄-induced HF mice. Inspired by the results of *in vivo* experiments, the anti-fibrosis effects of AHWE and the underlying mechanisms were studied *in vitro* as well.

The HSC-T6 cell line is a valuable cell model for studies of retinoid metabolism based on their similar retinoid phenotype as primary cell, which makes it an important tool for studying liver fibrosis *in vitro*. In addition, RAW264.7 is considered to be one of the best models of macrophages. These two different cell types could provide a guarantee for phenotypic verification and mechanism study. TGF- β 1 was used for directly stimulating the HSC-T6 cells to establish the *in vitro* liver fibrosis model, while LPS was employed to induce the RAW264.7 cells to establish the *in vitro* inflammation model as these are currently the relatively mature experimental modeling methods available for the cellular level (Dewidar et al., 2019) (Zhou et al., 2021). The potential cytotoxicity of AHWE toward these two types of cells was assessed using the CCK-8 assay kit. In the drug concentration range that had almost no effect on the cell viability in both cells, three appropriate drug concentrations were selected for evaluation in subsequent experiments. Consistent with the *in vivo* results, the immunohistochemical examination revealed that AHWE suppressed α -SMA expression. The changes in the expressions of the genes associated with fibrosis and inflammation, including *Acta2*, *Col1a1*, *Col3a1*, *Tnfa*, *Il6*, and *Il1 β* , were also significantly reversed upon AHWE treatment. It was observed that AHWE could inhibit the activation of HSCs and the inflammatory process. Among the various downstream signaling targets of HF, STAT and its family members, particularly STAT1 and STAT3 proteins, play an important role in the pathogenesis of HF. STAT3 is a transcription factor associated with the proliferation and activation of HSCs, and could, therefore, contribute to HF (Xu et al., 2014). In response to the cytokines and growth factors released upon liver injury, Janus tyrosine kinases phosphorylate STAT3, following which it dimerizes and translocates to the nucleus,

where it plays its role involving the transcriptional regulation of its target genes (Jatiani et al., 2010). The results of the present study indicated that LPS stimulation increased the p-STAT3 to STAT3 ratio relative to the control group in RAW264.7 cells. In addition, AHWE treatment decreased the protein expression levels of p-STAT3/STAT3 and the mRNA expressions of STAT3. Therefore, it was speculated that the inhibitory effect of AHWE on liver fibrosis was related to the activation of the STAT3 signaling pathway.

In the next experiment, STAT3 was overexpressed in the HSC-T6 and RAW264.7 cell lines using the pEGFP-STAT3 plasmid. Western blotting was performed to detect the STAT3 protein bands. The STAT3 protein levels were observed to be significantly higher in the plasmid transfected cells compared to the cells transfected with the empty vector. These results were validated in an independent cohort of samples using quantitative PCR. Therefore, it was inferred that the STAT3 overexpression cell line was successfully established. The expression levels of α -SMA protein, as revealed in the western blot analysis, validated that AHWE exerted an inhibitory effect on the TGF- β 1 stimulation-induced elevated SMA levels. However, the levels of the fibrosis marker α -SMA were significantly increased upon STAT3 overexpression, suggesting that STAT3 mitigated liver fibrosis. Furthermore, it was observed that the levels of *Acta2*, *Col1a1*, *Col3a1*, *Tnfa*, *Il6*, and *Il1 β* genes were significantly increased upon STAT3 overexpression, again suggesting that STAT3 mitigated liver fibrosis. These results further elucidated the mediating role of the STAT3 signaling pathway in the anti-fibrotic effect of AHWE *in vitro*. In order to verify the regulatory mechanism underlying this effect in mice that was consistent with the results of *in vitro* experiments, the expression levels of STAT3 in the liver tissue samples were determined using the immunohistochemical examination. The results presented in Figure 7A confirmed the upregulation of STAT3 expression in CCl₄-induced liver fibrosis tissue samples (tan-colored staining). This adverse effect was observed to decrease upon AHWE treatment. Moreover, the p-STAT3 to STAT3 ratio was increased in the CCl₄-induced HF mice, while the ratio was decreased upon AHWE treatment. The expression levels of the *Stat3* gene were determined in the liver samples. It was observed that *STAT3* expression was higher in the HF tissues than that in the normal liver tissues. In the presence of AHWE, the mRNA expression levels of this gene were decreased evidently in a dose-dependent manner (Figure 7C). The above results provided evidence that the regulation of the STAT3 signaling pathway was involved in the *in vivo* suppression of HF upon AHWE treatment.

5 Conclusion

The present study pioneered in demonstrating the potential anti-HF effects of AHWE. Moreover, it was

demonstrated these effects of AHWE were, at least in part, due to the inhibition of STAT3 signaling. The findings of the present study would serve as a strong pharmacological basis for designing a target-based therapy against HF, as well as for the utilization of AHWE as a novel phytotherapeutic agent in HF treatment.

Data availability statement

The original contributions presented in the study are included in the article/Supplementary Material, further inquiries can be directed to the corresponding authors.

Ethics statement

The animal study was reviewed and approved by Laboratory Animal Ethics Committee of Guangzhou University of Chinese Medicine.

Author contributions

LA, GZ, and SW contributed to conception and design of the study. BW, LH, YW, and LZ performed the experiments. BW wrote the first draft of the manuscript and performed the statistical analysis. All authors contributed to manuscript revision, read, and approved the submitted version.

Funding

This work was supported by The National Natural Science Foundation of China (82104687), The Basic and Applied Basic Research Fund Project of Guangdong Province (NO. 2019A1515110202), The Project of National Survey of Traditional Chinese Medicine Resources (GZY-KJS-2018-004) from National Administration of Traditional Chinese Medicine, The Fund for Improving Medical Service and Security Capacity of Department of Social Security, Ministry of Finance [(2019)39], and Guangdong Provincial Rural Revitalization Strategy Special Project - Guangdong Modern Southern Medicine Industry Technology System Innovation Team (2020KJ148).

Acknowledgments

We thank the International Institute for Translational Chinese Medicine of Guangzhou University of Chinese Medicine for technical assistance.

Conflict of interest

The authors declare that the research was conducted in the absence of any commercial or financial relationships that could be construed as a potential conflict of interest.

Publisher's note

All claims expressed in this article are solely those of the authors and do not necessarily represent those of their affiliated

organizations, or those of the publisher, the editors and the reviewers. Any product that may be evaluated in this article, or claim that may be made by its manufacturer, is not guaranteed or endorsed by the publisher.

Supplementary material

The Supplementary Material for this article can be found online at: <https://www.frontiersin.org/articles/10.3389/fphar.2022.1043022/full#supplementary-material>

References

- Adams, D. H., Ju, C., Ramaiah, S. K., Uetrecht, J., and Jaeschke, H. (2010). Mechanisms of immune-mediated liver injury. *Toxicol. Sci.* 115 (2), 307–321. doi:10.1093/toxsci/kfq009
- Barrientos, S., Stojadinovic, O., Golinko, M. S., Brem, H., and Tomic-Canic, M. (2008). Growth factors and cytokines in wound healing. *Wound Repair Regen.* 16 (5), 585–601. doi:10.1111/j.1524-475X.2008.00410.x
- da Silva Meirelles, L., Marson, R. F., Solari, M. I. G., and Nardi, N. B. (2020). Are liver pericytes just precursors of myofibroblasts in hepatic diseases? Insights from the crosstalk between perivascular and inflammatory cells in liver injury and repair. *Cells* 9 (1), 188. doi:10.3390/cells9010188
- Dewidar, B., Meyer, C., Dooley, S., and Meindl-Beinker, A. N. (2019). TGF-Beta in hepatic stellate cell activation and liver fibrogenesis—updated 2019. *Cells* 8 (11), 1419. doi:10.3390/cells8111419
- Ding, H., Yang, X., Tian, J., Wang, X., Ji, Y., El-Ashram, S., et al. (2021). JQ-1 ameliorates schistosomiasis liver fibrosis by suppressing JAK2 and STAT3 activation. *Biomed. Pharmacother.* 144, 112281. doi:10.1016/j.biopha.2021.112281
- Dong, H., Xian, Y., Li, H., Wu, Y., Bai, W., and Zeng, X. (2020). Analysis of heterocyclic aromatic amine profiles in Chinese traditional bacon and sausage based on ultrahigh-performance liquid chromatography-quadrupole-Orbitrap high-resolution mass spectrometry (UHPLC-Q-Orbitrap-HRMS). *Food Chem.* 310, 125937. doi:10.1016/j.foodchem.2019.125937
- Hillmer, E. J., Zhang, H., Li, H. S., and Watowich, S. S. (2016). STAT3 signaling in immunity. *Cytokine Growth Factor Rev.* 31, 1–15. doi:10.1016/j.cytogfr.2016.05.001
- Jatiani, S. S., Baker, S. J., Silverman, L. R., and Reddy, E. P. (2010). Jak/STAT pathways in cytokine signaling and myeloproliferative disorders: Approaches for targeted therapies. *Genes Cancer* 1 (10), 979–993. doi:10.1177/1947601910397187
- Kaiser, S. E., Brickner, J. H., Reilein, A. R., Fenn, T. D., Walter, P., and Brunger, A. T. (2005). Structural basis of FFAT motif-mediated ER targeting. *Structure* 13 (7), 1035–1045. doi:10.1016/j.str.2005.04.010
- Kany, S., Vollrath, J. T., and Relja, B. (2019). Cytokines in inflammatory disease. *Int. J. Mol. Sci.* 20 (23), 6008. doi:10.3390/ijms20236008
- Kim, H. J., Kim, S. Y., Shin, S. P., Yang, Y. J., Bang, C. S., Baik, G. H., et al. (2020). Immunological measurement of aspartate/alanine aminotransferase in predicting liver fibrosis and inflammation. *Korean J. Intern. Med.* 35 (2), 320–330. doi:10.3904/kjim.2018.214
- Latief, U., and Ahmad, R. (2018). Herbal remedies for liver fibrosis: A review on the mode of action of fifty herbs. *J. Tradit. Complement. Med.* 8 (3), 352–360. doi:10.1016/j.jtcme.2017.07.002
- Parola, M., and Pinzani, M. (2019). Liver fibrosis: Pathophysiology, pathogenetic targets and clinical issues. *Mol. Asp. Med.* 65, 37–55. doi:10.1016/j.mam.2018.09.002
- Ridner, S. H., Dietrich, M. S., Sonis, S. T., and Murphy, B. (2018). Biomarkers associated with lymphedema and fibrosis in patients with cancer of the head and neck. *Lymphat. Res. Biol.* 16, 516–524. doi:10.1089/lrb.2017.0074
- Tanwar, S., Rhodes, F., Srivastava, A., Trembling, P. M., and Rosenberg, W. M. (2020). Inflammation and fibrosis in chronic liver diseases including non-alcoholic fatty liver disease and hepatitis C. *World J. Gastroenterol.* 26 (2), 109–133. doi:10.3748/wjg.v26.i2.109
- Tarbit, E., Singh, I., Peart, J. N., and Rose-Meyer, R. B. (2019). Biomarkers for the identification of cardiac fibroblast and myofibroblast cells. *Heart fail. Rev.* 24 (1), 1–15. doi:10.1007/s10741-018-9720-1
- Trautwein, C., Friedman, S. L., Schuppan, D., and Pinzani, M. (2015). Hepatic fibrosis: Concept to treatment. *J. Hepatol.* 62 (1), S15–S24. doi:10.1016/j.jhep.2015.02.039
- Tsuchida, T., and Friedman, S. L. (2017). Mechanisms of hepatic stellate cell activation. *Nat. Rev. Gastroenterol. Hepatol.* 14 (7), 397–411. doi:10.1038/nrgastro.2017.38
- Villesen, I. F., Daniels, S. J., Leeming, D. J., Karsdal, M. A., and Nielsen, M. J. (2020). Review article: The signalling and functional role of the extracellular matrix in the development of liver fibrosis. *Aliment. Pharmacol. Ther.* 52 (1), 85–97. doi:10.1111/apt.15773
- Wang, Z., Li, J., Xiao, W., Long, J., and Zhang, H. (2018). The STAT3 inhibitor S3I-201 suppresses fibrogenesis and angiogenesis in liver fibrosis. *Lab. Invest.* 98 (12), 1600–1613. doi:10.1038/s41374-018-0127-3
- Wu, J., Lin, S., Wan, B., Velani, B., and Zhu, Y. (2019). Pyroptosis in liver disease: New insights into disease mechanisms. *Aging Dis.* 10 (5), 1094–1108. doi:10.14336/AD.2019.0116
- Wynn, T. A., and Ramalingam, T. R. (2012). Mechanisms of fibrosis: Therapeutic translation for fibrotic disease. *Nat. Med.* 18 (7), 1028–1040. doi:10.1038/nm.2807
- Xiang, D. M., Sun, W., Ning, B. F., Zhou, T. F., Li, X. F., Zhong, W., et al. (2018). The HLF/IL-6/STAT3 feedforward circuit drives hepatic stellate cell activation to promote liver fibrosis. *Gut* 67 (9), 1704–1715. doi:10.1136/gutjnl-2016-313392
- Xie, G. R., and Chen, H. J. (2021). Comprehensive betalain profiling of *djulis* (*Chenopodium formosanum*) cultivars using HPLC-Q-orbitrap high-resolution mass spectrometry. *J. Agric. Food Chem.* 69 (51), 15699–15715. doi:10.1021/acs.jafc.1c06596
- Xu, M. Y., Hu, J. J., Shen, J., Wang, M. L., Zhang, Q. Q., Qu, Y., et al. (2014). Stat3 signaling activation crosslinking of TGF- β 1 in hepatic stellate cell exacerbates liver injury and fibrosis. *Biochim. Biophys. Acta* 1842 (11), 2237–2245. doi:10.1016/j.bbdis.2014.07.025
- Yang, Y. M., and Seki, E. (2015). TNF α in liver fibrosis. *Curr. Pathobiol. Rep.* 3 (4), 253–261. doi:10.1007/s40139-015-0093-z
- Yu, H., Pardoll, D., and Jove, R. (2009). STATs in cancer inflammation and immunity: A leading role for STAT3. *Nat. Rev. Cancer* 9 (11), 798–809. doi:10.1038/nrc2734
- Zhou, M., Tang, Y., Liao, L., Liu, M., Deng, Y., Zhao, X., et al. (2021). Phyllygenin inhibited LPS-induced RAW 264.7 cell inflammation by NF- κ B pathway. *Eur. J. Pharmacol.* 899, 174043. doi:10.1016/j.ejphar.2021.174043

Glossary

Aps ammonium persulfate

Acta2 actin alpha 2

AH *Amydrium hainanense* (H.Li, Y.Shiao & S.L.Tseng) H.Li

AHWE water extract of *Amydrium hainanense* (H.Li, Y.Shiao & S.L.Tseng) H.Li

ALT alanine transaminase

α -SMA alpha smooth muscle actin

AST aspartate transaminase

BCA bicinchoninic acid assay

CCl₄ Carbon tetrachloride

Col I collagen 1

Col III collagen 3

Col1a1 collagen 1a1

Col3a1 collagen 3a1

DAB Diaminobenzidine tetrahydrochloride

DMEM Dulbecco's modified eagle medium

DMSO Dimethyl sulfoxide

ECL enhanced chemical luminescence

EDTA ethylenediaminetetraacetic acid

ECM extracellular matrix

FBS Fetal bovine serum

GAPDH glyceraldehyde-3-phosphate dehydrogenase

H&E hematoxylin and eosin

HF hepatic fibrosis

HSCs hepatic stellate cells

LPS lipopolysaccharide

IL-1 β interleukin-1 beta

IL-6 interleukin-6

PAGE polyacrylamide gel electrophoresis

PBS phosphate buffer Saline

PVDF polyvinylidene fluoride

SDS sodium dodecyl sulfate

STAT3 signal transducers and activators of transcription 3

TBS Tris buffered saline

TEMED N, N, N', N'-Tetramethylethylenediamine

Tris Tris (hydroxymethyl) aminomethane

TNF- α tumor necrosis factor- α

TGF- β 1 transforming growth factor beta 1